PARTICLE STREAK VELOCIMETRY OF SUPERSONIC NOZZLE FLOWS

J. D. Willits and T. L. Pourpoint

Purdue University

West Lafayette, IN

ABSTRACT

A novel velocimetry technique to probe the exhaust flow of a laboratory scale combustor is being developed. The technique combines the advantages of standard particle velocimetry techniques and the ultra-fast imaging capabilities of a streak camera to probe high speed flows near continuously with improved spatial and velocity resolution. This “Particle Streak Velocimetry” technique tracks laser illuminated seed particles at up to 236 picosecond temporal resolution allowing time-resolved measurement of one-dimensional flows exceeding 2000 m/s as are found in rocket nozzles and many other applications. Developmental tests with cold nitrogen have been performed to validate and troubleshoot the technique with supersonic flows of much lower velocity and without background noise due to combusting flow. Flow velocities on the order of 500 m/s have been probed with titanium dioxide particles and a continuous-wave laser diode. Single frame images containing multiple streaks are analyzed to find the average slope of all incident particles corresponding to the centerline axial flow velocity. Long term objectives for these tests are correlation of specific impulse to theoretical combustion predictions and direct comparisons between candidate green fuels and the industry standard, monomethylhydrazine, each tested under identical conditions.

α	=	time constant for spheres in Stokes drag	[s]
β	=	oblique shock angle	[°]
d	=	diameter	[m]
Isp	=	specific impulse	[s]
n	=	correction factor for Stokes drag at high Reynolds number	[-]
O/F	=	oxidizer to fuel mass flow ratio	[-]
P_0	=	stagnation pressure	[psia]
ρ	=	density	[kg/m^3]
ϕ	=	particle to flow velocity ratio	[-]
Re	=	Reynolds number	[-]
r	=	radius	[mm]
T_0	=	stagnation temperature	[K]
Δt	=	time step	[s]
t_s	=	temporal scaling factor	[µs/pixel]
θ	=	streak angle	[°]
μ	=	dynamic viscosity	[Pa-s]
u	=	velocity	[m/s]
x	=	nozzle position	[mm]
y_s	=	spatial scaling factor	[µm/pixel]
λ	=	dimensionless parameter from 2nd order ODE solution	[-]
f	=	fluid subscript	
p	=	particle subscript	

INTRODUCTION

Toxicity, high vapor pressure, and the corrosive properties of typical monopropellants and hypergolic propellants in use today add significant cost and risk to their application in spacecraft and missile propulsion needs. To increase the safety in operating with these propellants while meeting existing performance standards, work at Purdue University has focused on less-toxic alternatives. Data acquired since 2013 with hypergolic propellants in a small laboratory combustor allows for calculation of ignition delay and characteristic velocity for a diverse field of alternative and standard propellants.[1] By

identifying rapidly igniting propellants and comparing predictive performance to measured, positive trends in propellant synthesis can be identified and further studied. Current work focuses on amine-borane compounds being developed in conjunction with the Purdue Chemistry Department.[2] A leading candidate is triethylamine borane as it offers ignition delays as low as 3 ms, low vapor pressure, and an NFPA health rating of 3.

The addition of a specific impulse (*Isp*) measurement would aid in further confirming or rejecting theoretical claims of a propellant's performance. While taking thrust and mass flow data is the typical method to achieve this, geometric limitations in the injector system described by Willits et al. preclude the installation of an in-line load cell. Therefore, the work here details developmental testing aimed at providing an optical method for determining nozzle exhaust velocity which can similarly be converted to Isp without altering the injection system.

BACKGROUND

Several options exist to obtain a flow velocity measurement.[3] Intrusive methods include hotwire anemometry, Pitot-static probes, and turbines among others. Due to material constraints, these are likely not viable for high temperature and corrosive flows characteristic of rocket nozzles. Non-intrusive (or minimally so) methods rely on optical techniques often involving high speed cameras and powerful lasers. Examples include: Schlieren imaging where density gradients can be visualized by passing a collimated beam through the flow, Doppler where the spectral shift from a stimulated flame emission or an illuminated particle is recorded, and visual particle tracking techniques such as Particle Image Velocimetry (PIV) where a seed material is added to the flow and illuminated.

A key distinction in these non-intrusive methods is the requirement of known flow composition. Shock waves observed by Schlieren can provide Mach number which requires molecular composition and temperature information to convert to velocity. Doppler methods using laser excitation techniques such as Raman spectroscopy are referenced to emission wavelengths of specific species in the exhaust. In contrast, seeded techniques require less stringent knowledge of flow properties making them more ideal for investigation of wholly new propellant formulations. Particles must simply be sized such that the velocity lag relative to length and time scales in the flow of interest is sufficiently small. Provided that background flame emissions can be filtered out from the seed signal, seeded techniques can be applied in the exact same manner irrespective of the exhaust plume composition.

While non-seeded techniques require more information than seeded techniques, some, such as Doppler, become more resolvable as velocity increases. Conversely, velocities of seeded flows have an upper limit based on the system. In PIV, the maximum velocity is governed by the window length and the time step between frames. A conventional limitation of PIV to avoid aliasing is that the particle displacement across one frame pair must be at least four times smaller than the interrogation windows.[4] Pulsed illumination sources can easily reach down to sub-nanosecond separation time, but the shutter speed of commercially available, cutting-edge cameras used to image such flows is typically limited to between 100 and 500 ns.[5,6,7] The measured velocity is averaged across an entire window meaning that constant or linearly accelerating flows produce accurate mean values at the window center location. However, this is not valid for flow fields with high velocities and non-linear acceleration in the direction of the flow; both of which are characteristic of rocket exhaust flows. At times scales of 100 to 500 ns, the interrogation window size required to accurately resolve the magnitude and position of velocity vectors without aliasing becomes prohibitively small.

A novel adaptation of PIV using a streak camera is posited to provide superior velocity limits at the spatial scales required for the exhaust measurement described above. Streak cameras are used to track objects at high velocity in one spatial dimension. On a single frame, the signal on the y-axis is swept across the x-axis at a controlled rate and the time step is governed by the dwell time on each pixel.[8] Velocity is calculated from the slope of this line. While traditionally applied to macroscopic objects such as projectiles[9] and detonation waves[10] or to dispersed spectra[11] of reacting fields, the proposed technique, called Particle Streak Velocimetry (PSV), uses a digital streak camera to track small seed particles and infer 1-D flow velocity. Frame straddling with the need for post-processing of interrogation windows is

eliminated. This yields potential improvements in spatial resolution and time resolved data. Use of a continuous light source rather than a dual-pulsed system can reduce syncing requirements and possibly cost. Seeding density can be lowered as each particle is a sample rather than each filled window. While not a considerable impact in most situations, seed does remove momentum from the carrying flow and a reduction of this effect would reduce intrusion of the measurement. The auxiliary flow rate needed to introduce the seed may also be reduced which could preserve the chemical composition in a reacting flow.

The ability to track particles near continuously would improve temporal resolution over current state of the art. In traditional PIV, cameras with sufficient shutter speed can be acquired with sample rates exceeding 1 MHz (at drastically reduced resolution); however, most pulsed laser systems are limited to the 10 kHz range. Experimental work is underway to provide 500 kHz[12] or even 1 MHz[13] pulse trains in a pursuit of Time-Resolved PIV (TR-PIV). By comparison, the system utilized in this work can operate with effective 1-D sampling rates from 40 kHz up to 4.2 GHz. While not necessary for this intended *Isp* measurement, such capability may hold applications both to further investigations in this work and many other topics requiring time resolution of this scale and/or exceedingly high velocities including energetic materials reaction fronts, hypersonic combustion, and supersonic aerodynamics among others.

APPROACH METHODOLOGY

TEST ARTICLE

A supersonic nozzle test bed was developed to demonstrate PSV and validate it against predictions and an existing technique, Schlieren imaging. The system runs on high purity compressed gas. With the facility bulk nitrogen or a gas cylinder, testing can be performed rapidly and indefinitely as opposed to the several hours of setup and cleaning required for a single two second firing with propellants. Cold gases have much lower sonic velocities than bipropellant rocket exhausts to allow initial proof of concept and troubleshooting under less stringent conditions. This also gives the ability to easily increment the velocity via selecting gases of different molecular weights such as nitrogen, argon, and helium. By using single composition gases, the expected velocities from fundamental principles are easily determined as opposed to a complex field of unknown and continuously reacting products. The elimination of background light emission present with combustion reduces the power and filtering needs for the illumination source and collection optics. The introduction of the seed particles to the main flow is also simplified as they can be injected to the bulk flow far upstream of the nozzle. In a combusting environment, geometric, environmental, and chemical restrictions will complicate the seeding process. Melting point and chemical compatibility of the seed will need to be addressed as well as whether to inject it into the chamber inert gas flow or by suspending it in the liquid propellants prior to injection.

The nozzle, shown in Figure 1, is machined from stainless steel 304 with a 0.183 inch throat and an expansion ratio of 1.5 at the exit. It interfaces with a combustion chamber used for prior hypergol characterization research[1] which will be the target measurement destination after this proof of concept. For cold gas testing, the holder is made from aluminum and contains a 2.5 inch long by 0.735 inch diameter settling region to measure stagnation temperature and pressure and to allow the bulk and seeder flow to straighten before reaching the nozzle. The seeder, shown in Figure 2, is adapted from a design by DLR[14] using a sintered disk to produce the fluidized seed bed in a 3 inch pipe. A sonic orifice of 0.021 inch is used to limit the flowrate and to control the gas velocity in the pipe relative to the particle terminal velocity. For initial testing, titanium dioxide was selected as the seed material due to its wide availability in sub-micron sizes, high refractive index, low cost, and relatively high melting temperature of 2100 K. The sample was acquired from Evonik Industries labeled Aeroxide P 25.

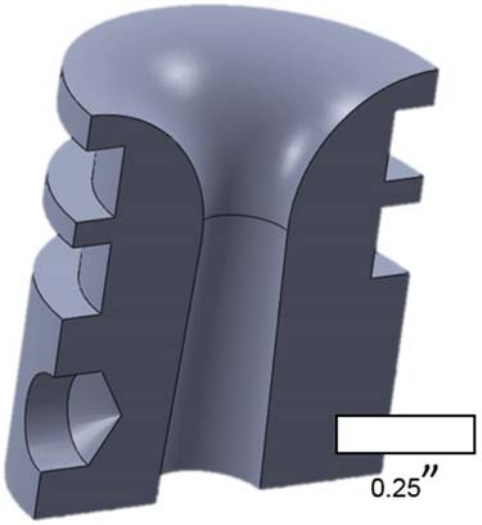

Figure 1. Expanding Supersonic Nozzle with 0.183 inch Throat and Expansion Ratio of 1.5

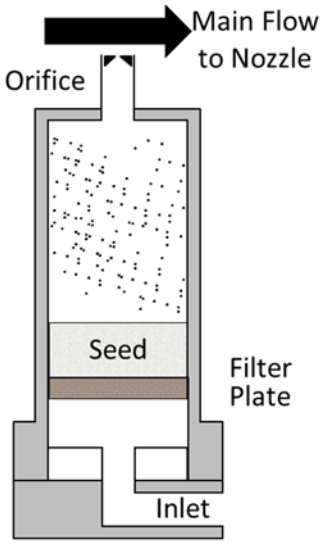

Figure 2. Seeder Diagram

MEASUREMENT SYSTEM

Modern streak cameras record images by directing the incident light onto a photocathode which outputs electrons. These are diverted via a changing electric field inside a streak tube. The rate at which the field changes governs the temporal axis of the resulting data. A micro-channel plate (MCP) multiplies these electrons which are then converted back to photons by a phosphor screen. This image is then captured by a CCD with one axis indicating space and the other time.[15] Because the electric field can be swept across each pixel much more quickly than a traditional high speed shutter can cycle, extremely fine temporal resolutions can be achieved at the cost of one spatial axis. The Sydor Instruments Ross 2000 used for this study provides recording times from 30 ms to 300 ns with 25 μs and 236 ps resolution, respectively.[16]

The elimination of the shutter allows PSV to be performed with a continuous light source as opposed to the frame straddling of dual pulse lasers used in PIV. The developmental system described here uses a 1.6 Watt, 445 nm laser diode with a 2 Amp switching DC power supply. The MCP integrated into the streak camera provides a lower detection threshold than CCD or CMOS detectors alone. For eventual measurements with higher background noise, such as a rocket plume, a more powerful laser source with line filters will be necessary.

Figure 3 shows a diagram of the test article and measurement setup. The diode is oriented with the linearly polarized axis vertically oriented. The output is formed into an expanding sheet using a collimating lens and a cylindrical lens. The horizontal waist is located at the nozzle center line with the sheet height being approximately 5 mm and positioned at the nozzle exit plane. A spherical lens and micrometer slit act as a field stop to limit the width of the axial line being imaged. This allows further control of the number of particles being imaged and the total light intensity. A dovetail prism rotates the image 90° to align with the streak camera photocathode orientation. A 200 mm f/4 macro Nikon lens is used to capture the image. As delivered, the system includes a UV-Vis spectrometer, but for the purposes of this experiment, this is bypassed by setting the diffraction grating to a zero-order reflection which will act as a plane mirror directing the signal into the streak camera.

1) 445 nm Laser Diode with Focusing Lens
2) Positive Cylindrical Lens
3) Beam Dump
4) Positive Spherical Lens
5) Micrometer Slit
6) Dovetail Prism (90° Rotation)
7) 200 mm Macro Lens
8) Spectrometer in Zero-Order Reflection Position
9) Streak Camera

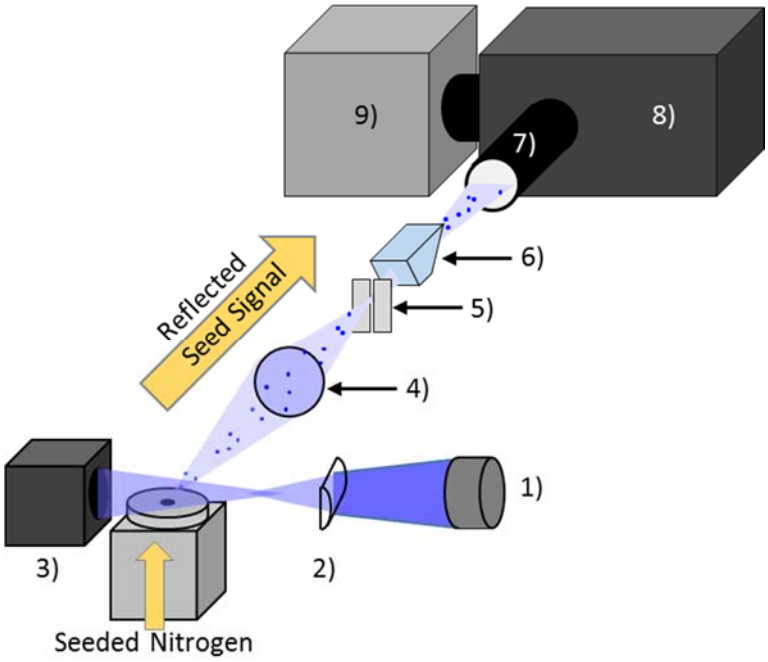

Figure 3. Compressed Gas Test Bed Schematic

FOCUS AND CALIBRATION

Focusing the streak image with only one spatial dimension is accomplished by identifying sharp peaks in the vertical line output and maximizing signal intensity for a given aperture, slit, and laser power setting. A vertical wedge, shown in Figure 4, is positioned at the nozzle axis, and the laser sheet is aimed down the perpendicular channel to the tip. To provide a steady, miniscule object while setting the working distance, the wedge is replaced with a thin wire inserted diagonally into the midpoint of the laser sheet and rotated until the reflection is shown imaged on the closed micrometer slit which is then fully opened. Figure 5 shows the raw image of the wire swept across the time axis at some arbitrary speed to provide sufficient intensity for this process. Figure 6 shows the time-averaged intensity with respect to vertical position, typically referred to as “line-out”, from the center portion of the raw image. The full width at half maximum is 10 pixels which correlates well with the expected minimum resolution derived from the quoted streak tube resolution of 10 line pairs per millimeter at 40% contrast and pixels of 6.45 μm. Once the lens is focused, the wedge is again installed to determine the spatial magnification. Shims, each 1/32 inch thick, are stacked in front of the wedge to successively block the reflected beam and find a spatial scaling factor to dimensionalize the captured streaks. A value of 16.4 μm/pixel is used for tests reported in this paper.

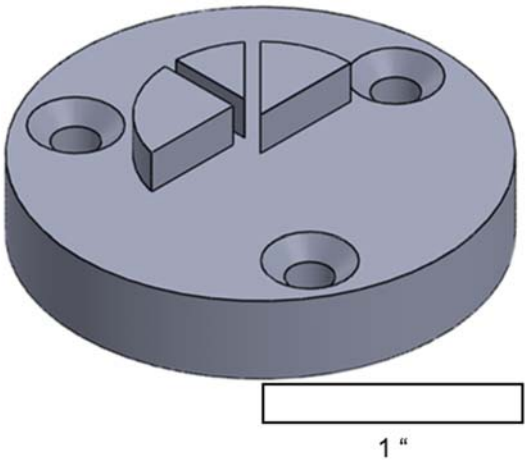

Figure 4. Alignment Wedge

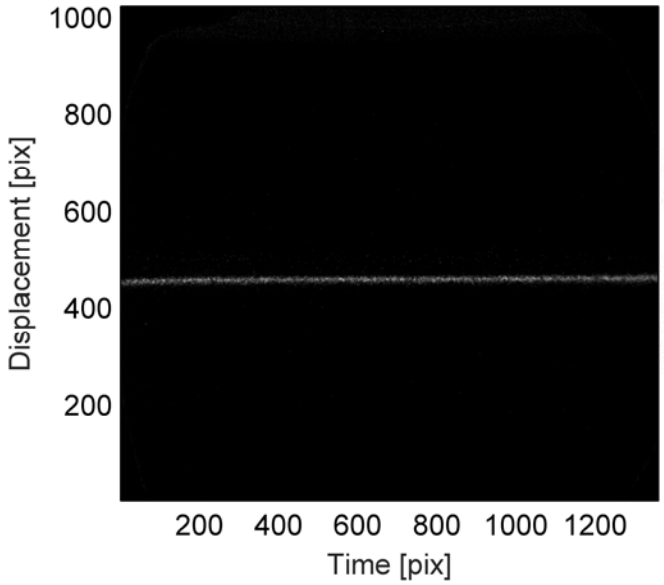

Figure 5. Focusing Wire Raw Image

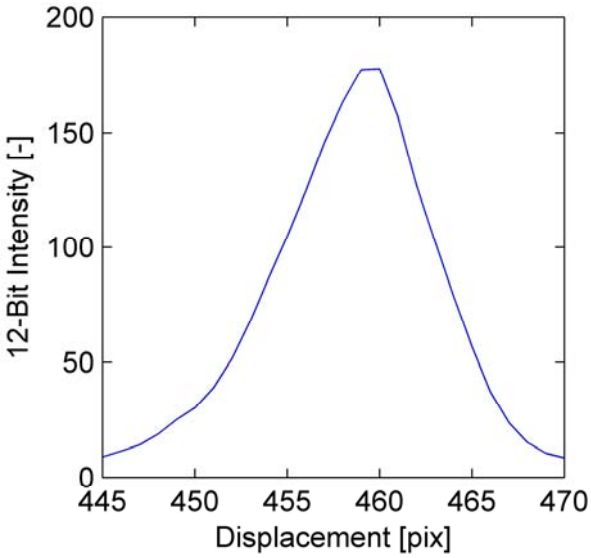

Figure 6. Focusing Wire Vertical Lineout

PARTICLE LAG

Velocity lag contributes to uncertainty and dictates the length scale of resolvable features such as shocks, boundary layers, or eddies. In regards to this experiment, the length of the nozzle must be proven adequate to accelerate the particle to a sufficient fraction of the exit velocity. Seed particle density and diameter must be carefully selected as they impact the acceleration under Stokes flow along with fluid properties. Gilbert[17] describes how particle response to a general flow field can be modeled by iterative application of Stokes drag along a 1-D, linearly accelerating flow. While the method described by Gilbert simply split a Mach curve into three linearly accelerating components, a higher fidelity solution can now be found using a forward stepping solver which calculates gas velocity and instantaneous acceleration along with other fluid properties at each x location. In Equations 1-6 below, uf and up represent the flow and particle velocities. The time constant α is derived from Stokes flow, and n is a correction factor for the Stokes drag at increased Reynolds number. Equations 1 and 6 are used to advance the particle down the nozzle. The time step must be small enough to approximate the velocity gradient in Equation 3 as constant.

$$u_{p_i} = e^{-\frac{\Delta t}{\alpha}}\left[u_{p_{i-1}}\, cosh\left(\frac{\Delta t\lambda}{\alpha}\right) + \frac{2u_f - u_{p_{i-1}}}{\lambda}\, sinh\left(\frac{\Delta t\lambda}{\alpha}\right)\right] \quad (1)$$

$$\lambda = \sqrt{1 + 2\alpha\, \frac{du_f}{dx}} \quad (2)$$

$$\alpha = n\frac{\rho_p d_p^2}{9\mu} \quad (3)$$

$$n = \begin{cases} \dfrac{150}{175Re^{.15} + 3Re}, & if\ Re > 1 \\ 1, & otherwise \end{cases} \quad (4)$$

$$Re = \frac{\rho_f d_p}{\mu}(u_f - u_{p_{i-1}}) \quad (5)$$

$$x_i = x_{i-1} + u_{p_i}\Delta t \quad (6)$$

For a given nozzle geometry, the gas velocity is solved numerically by the area ratio at each location assuming 1-D isentropic flow with knowledge of flow stagnation temperature and ratio of specific heats. For tests with pure nitrogen this is easily done, however, expanding these predictions or implementing velocimetry techniques requiring the ratio of specific heats, such as Schlieren, to reactive flows with changing product composition introduces tremendous uncertainty. Therefore, the present analysis provides only an order of magnitude of the velocity uncertainty to select particle diameter and density. Simulations were run for TiO_2 particles of 0.4 μm diameter with geometry of the current nozzle design for measured stagnation temperature with nitrogen and ratio of specific heats of 1.4. Necessary data for monomethylhydrazine (MMH) and red-fuming nitric acid (RFNA), an industry standard hypergolic fuel/ox pair, was predicted using CEA assuming a chamber pressure of 200 psia and an oxidizer-to-fuel ratio of 2.2. The model was initiated with ϕ =1 at the beginning of the nozzle contraction. The estimated ratio of particle to flow velocity at the exit exceeded 98% in each case, as shown in Figure 7 and Figure 8. A 2% error is suitable for this study if these ideal conditions can be met, and the option remains for improvement via altered nozzle geometry and smaller particle size if necessary. The area of greatest particle lag is found just after the throat. The faster, reacting flow actually performs better due to viscosities almost an order of magnitude higher than the cold nitrogen. The discontinuity at position 0 is where the area ratio-Mach number solver transitions from subsonic to supersonic and does not greatly affect the predicted flow or particle velocity.

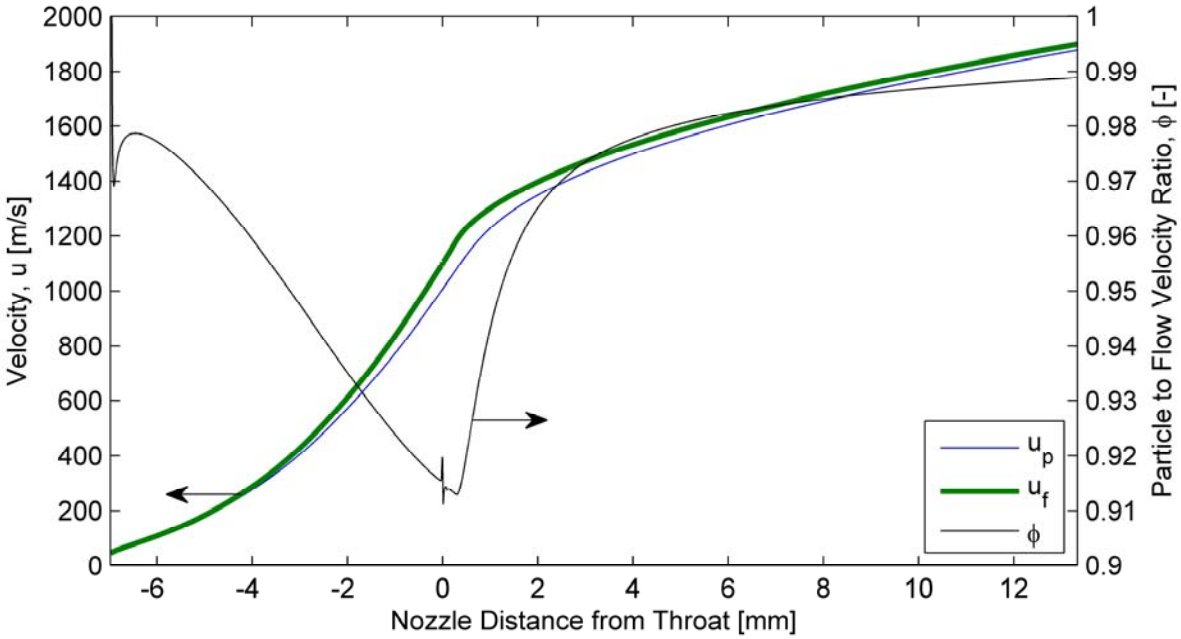

Figure 7. Particle (u_p) and Fluid (u_f) Velocity in MMH/RFNA Exhaust through the Nozzle (d_p=0.4 µm, P_0 = 200 psia, T_0 = 3000 K, O/F =2.2)

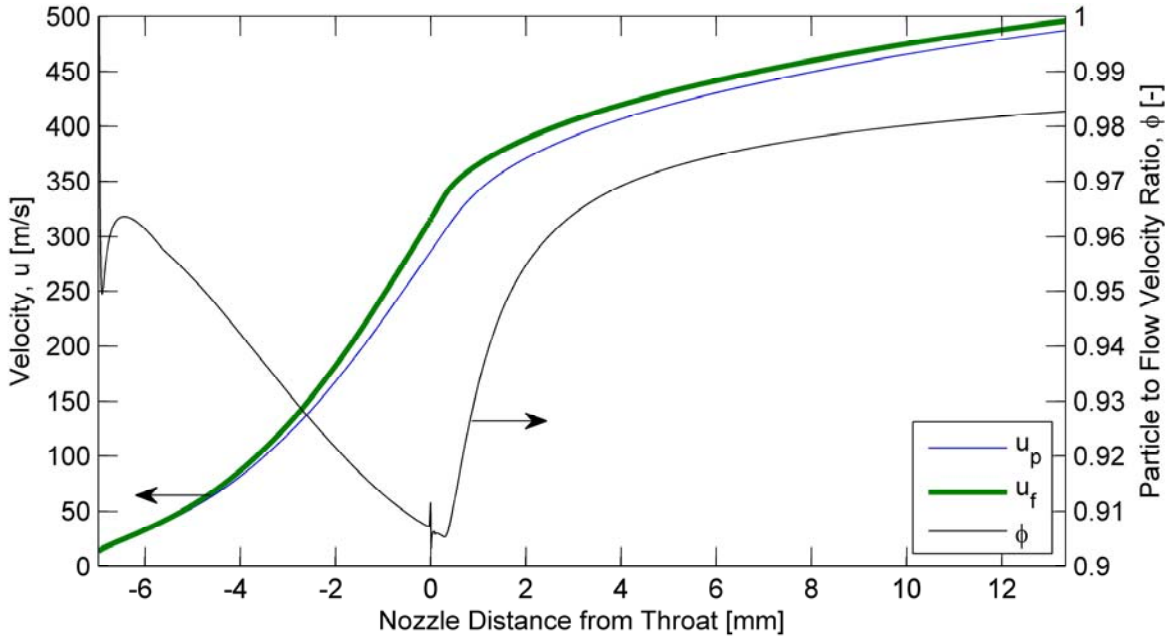

Figure 8. Particle (u_p) and Fluid (u_f) Velocity in Nitrogen through the Nozzle (d_p=0.4 µm, P_0 = 115 psia, T_0 = 285 K)

IMAGE PROCESSING

While the eventual goal of this technique is to provide 1-D spatially and temporally resolved flow velocity data, this initial testing is assumed to be measuring a field at steady state which is small enough to ignore spatial variance. This allows the CCD frames captured by the streak camera to be analyzed as

one whole image rather than locating and analyzing individual streaks. This greatly reduces the need for filtering out signal noise and is much more forgiving for out of focus particles and varying intensity through the laser sheet. The region of interest is cropped from the 1024x1360 pixel, 12-bit, raw image, shown in Figure 9, and is then padded to 1360x1360. The current setup has a field of view limited to approximately 200 pixels in the y direction due to the inline spectrometer.

A 2-D Continuous Space Fourier transform (CSFT) is performed, shown in Figure 10, and the horizontal spatial component (center vertical stripe in CSFT) is removed by taking the mean of points on either side. The center 400x400 pixels are cropped to isolate the diagonal peak which is orthogonal to the dominating orientation of all components in the spatial field, i.e. the diagonal streaks. The baseline is linearized using a piecewise cubic interpolation function across each row and then across each column. A generic 2-D Gaussian profile is then fit to this data, shown in Figure 11, using a least squares solver for non-linear functions.[18] This value can be fit to the velocity by Equation 7 where θ is the best fit orientation parameter from the Gaussian profile solver, and y_s and t_s are the spatial and temporal scaling factors from pixels to millimeters and microseconds.

$$u_p = \tan\theta \, \frac{y_s}{t_s} \tag{7}$$

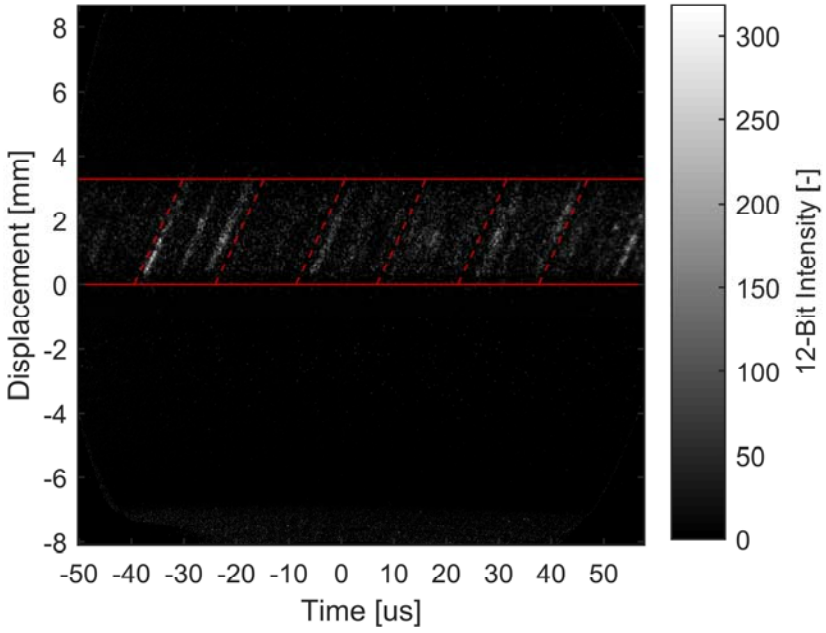

Figure 9. Raw Streak Image Overlain with ROI (Solid) and Average Streak Orientation (Dash)

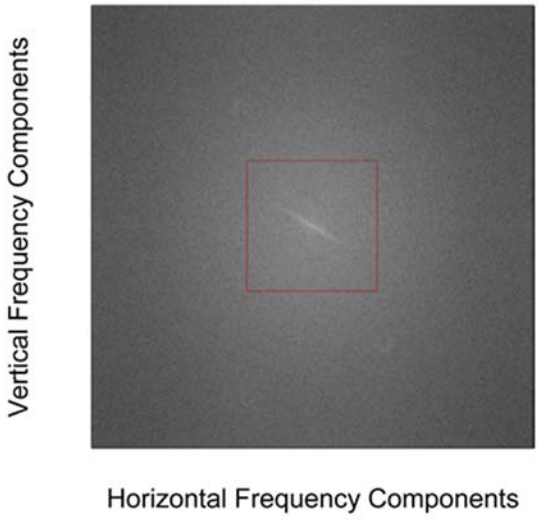

Figure 10. Full Scale Raw CSFT with ROI

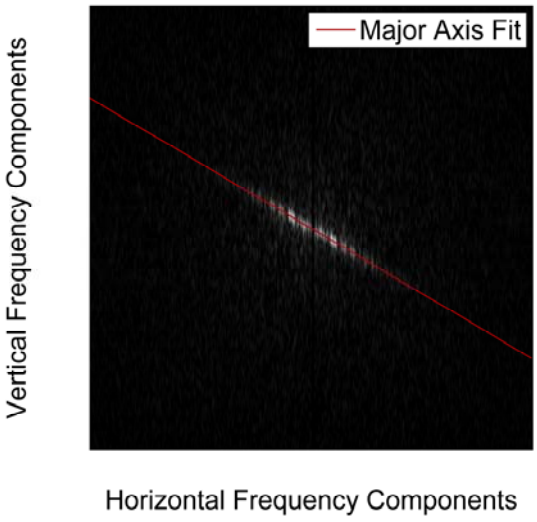

Figure 11. Cropped, Linearized CSFT with Orientation Fit

RESULTS AND DISCUSSION

Tests were run with a stagnation pressure of 115 psia and a seeder pressure of 315 psia. Aperture and laser power were incrementally increased to achieve sufficient image intensity while being cautious not to overload the MCP though the full settings for each were eventually reached. Sweep speed was varied to produce resolvable slopes that avoid nearly vertical or horizontal streaks, and the slit width was varied to increase the measurement field which raises the particle sampling frequency at the faster sweep speeds. Sweeps in the range of 50 to 100 µs yielded favorable results which are shown in Table 1, and the slit width varied from 0.5 to 1.5 mm. Measured stagnation temperature ranged from 285 to 288 K. This corresponds to a change in expected fluid velocity of around 1 m/s per K. Tests 1 through 6 exhibited between 5 and 20 distinct streaks while multiple attempts at the 10 µs sweep speed yielded only test 7 with a single visible streak. Increased seeding density will be discussed in the future works section. Neglecting test 7 due to its low number of samples, the mean velocity is 354 m/s with a standard deviation of 7 m/s. The calculated uncertainty from Equation 7 is 6% based on the precision of the spatial and time scaling factors.

Table 1. Summary of Nitrogen Cold Gas PSV Tests

Test Number	Sweep Speed [µs]	T_0 [K]	θ [°]	u_p [m/s]	Isentropic u_f [m/s]	ϕ [-]
1	50	287	40.5	356	493	0.721
2	50	288	41.5	369	494	0.748
3	100	287	59.3	348	493	0.706
4	100	286	59.5	351	492	0.713
5	100	285	59.5	351	491	0.715
6	50	285	39.9	349	491	0.710
7	10	285	8.8	319	491	0.650

Two factors are suspected sources of the large disparity in measured and expected particle lag: binding of the seed particles and real fluid effects. Both moisture and inter-particle effects such as static charge can cause the seed particles to form larger agglomerates over time. The nominal size is on the order of 0.3 µm, but analysis using the code discussed in the “Particle Lag” section of above shows that a particle on the order of 3 µm would reach 350 m/s given the same flow conditions. While this code is not

meant for detailed quantitative analysis, it is plausible that, given the current seeder geometry, clusters of this size could be formed. Currently, the only agitation is from the flow itself.

Likewise, the isentropic flow calculations predicting the gas velocity may provide a biased target due to viscous, thermodynamic, geometric inaccuracies, and other factors. For this reason, Schlieren imaging of the exhaust plume was performed to better estimate the true exit velocity using existing techniques. Because the nozzle is slightly under-expanded under the given operating and ambient conditions, oblique shock wave theory can provide an estimation of the true Mach number.[19] By measuring the angle of the incident and reflected shock from the centerline, visualized in Figure 12 as β_1 and β_2, and following the assumption that the flow enters the first shock and exits the second shock purely in the axial direction, a unique solution for the upstream Mach number can be found. Again this requires information about the chemical composition of the gas making it only useful as a check in these idealized tests and not for future applications with reacting flows. High speed videos were taken of the nozzle with a stagnation pressure of 115 psia at 25,000 fps, 144x368 resolution, and 1-to-1 magnification using a Phantom v7.3 camera. The incident angles were found to be 147.2° and 33.1° resulting in an observed Mach number of 1.85 at the nozzle exit. The exit Mach number predicted from the listed nozzle geometry and isentropic flow analysis is also 1.85. Combined with the measured stagnation conditions of the seeded flow tests, this finding serves to prove the predicted flow velocity of 491 m/s to be accurate. The large disparity in predicted to measured particle lag is due to real effects in the particle behavior pointing most likely to larger diameter agglomerates forming in the seeder rather than non-isentropic losses of the fluid itself inside the nozzle.

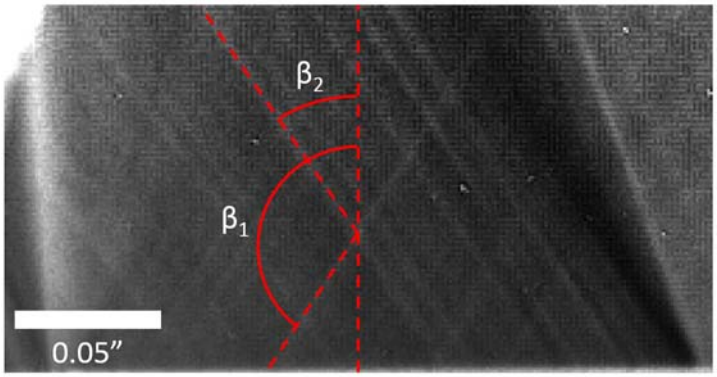

Figure 12. Schlieren Image of Reflected Oblique Shocks at the Nozzle Exit

SUMMARY AND CONCLUSIONS

A new process to measure high speed, seeded flows was introduced. Particle Streak Velocity can increase the measurable velocity of traditional PIV as well as provide time resolved sampling in certain applications, such as rocket exhaust flows, at the cost of one spatial axis. A test bed to develop the technique at velocities below 500 m/s with non-reacting flows of known composition was created. A seeder was built, and a seed flow-following behavior analysis was performed. TiO_2 particles on the order of 0.4 μm were found to introduce less than a 2% velocity lag in the predicted flow. An image processing algorithm was developed to analyze the entire sample as a steady-state, spatially-independent measurement. Tests were conducted at identical conditions using compressed nitrogen and the mean particle velocity at the nozzle exit was found to be 354 m/s with a standard deviation of 7 m/s. This is compared to an expected value from both isentropic flow principles and analysis of the plume shocks via Schlieren of 491 m/s. The discrepancy is attributed to likely agglomeration of the seed particles within the seeder. A solution to ensure proper seed size will be implemented as well as further investigation of this velocimetry technique’s limits and applications.

FUTURE WORK

As described in the “Results and Discussion” section, the most pressing matter is to characterize the actual size of particles leaving the seeder and to reduce that to sizes necessary to follow the flow at sufficiently low velocity lag. Verification of the real particle sizes will be done by capturing samples on tape at the nozzle exit and examining with a desktop SEM. The sonic orifice used to control the pipe velocity will be resized to carry particles only smaller particles and an agitation method such as that described by Willert[20] will be considered. Smaller samples of titania may be acquired or different materials may replace it all together to reduce agglomeration. Once more reliable flow following capability of the seed is achieved, the testing described here will be expanded to new conditions via altered nozzle geometry or different compressed gases to increment the velocity and further extend the capabilities of PSV.

Improvements will be made to the image analysis algorithm. A goodness of fit metric for the Gaussian solver will be determined to differentiate tests with more consistent slopes among all streaks. This will likely involve the width of the solved profile with narrower peaks showing tighter grouping along with data fed back from the solver for metrics such as residuals, iterations required, and specified tolerance. In parallel, an adaptation or a wholly new method to analyze the plots will be developed to allow spatially and temporally resolved analysis of a single frame. This would involve tiling the frame into smaller interrogation windows and thus will likely require higher seeding densities and spatial resolution to provide more streak samples within a given frame. In part this will be achieved by removing the spectrometer to open the field of view to the entire CCD spatial axis.

The intention of this proof of concept is to prepare the PSV technique to be applied in the exhaust plume of a laboratory-scale hypergolic thruster used for characterizing novel green propellants.[1] By measuring the exhaust velocity with a known mass flow rate, specific impulse of candidate propellants can be measured and compared to industry standard options. The combustor has been outfitted with a borosilicate tube allowing direct visualization of the nozzle exit as shown in Figure 13. Future work will take place to adapt the collection optics from the optical table to the injector stand. A more powerful continuous wave laser will be acquired to overcome the background noise introduced by the combustion products. The wavelength must be chosen to avoid any strong emission lines of likely products so that a line filter can be applied to isolate only the signal reflected from the seed. This will require some preliminary spectroscopy work using the Princeton SpectraPro 2300 currently integrated with the streak camera.

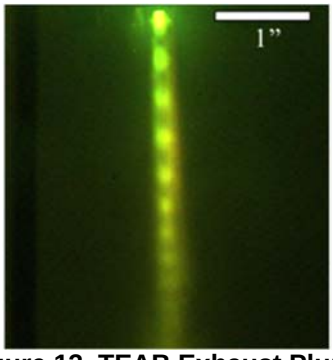

Figure 13. TEAB Exhaust Plume

Chemical compatibility and suspension stability tests will be performed to investigate seeding the liquid propellants before injection rather than via a fluidized bed as used for this test. In the event that an acceptable solution cannot be found, the current seeder will be adapted to interface with the chamber and resized to suit the seeding requirements of such tests. Preliminary tests have shown no visible reaction between the titania and liquid MMH.

ACKNOWLEDGMENTS

This work was supported by a NASA Space Technology Research Fellowship.

REFERENCES

1 J.D. Willits, J.D. Dennis, A.S. Kulkarni, P.V. Ramachandran, T.L. Pourpoint, Combustion Characterization of Amine Borane Hypergolic Propellants, 50th AIAA/ASME/SAE/ASEE Joint Propulsion Conference, Cleveland, OH, AIAA 2014-3884, 2014.

2 P.V. Ramachandran, A.S. Kulkarni, M.A. Pfeil, J.D. Dennis, J.D. Willits, S.D. Heister, S.F. Son, T.L. Pourpoint, *Amine-Boranes: Green Hypergolic Fuels with Consistently Low Ignition Delays*, Chemistry: A European Journal, Vol. 20, Issue 51 (2014), pp. 16869-16872.

3 Physical Measurements in Gas Dynamics and Combustion

4 PIV practical guide

5 Vision Research, Phantom UHS-12 Series, Phantom v2512 datasheet, Oct. 2015.

6 Photron, FASTCAM SA-X2 High Performance High-Speed Camera System, SA-X2 datasheet, Oct. 2015.

7 LaVision, Image sCMOS, sCMOS datasheet, Oct. 2015.

8 Hamamatsu, Guide to Streak Cameras, July 2014.

9 Projectile streak camera

10 Detonation wave streaks

11 Spectra streaks

12 25 kHz

13 1 MHz

14 C. Willert, G. Stockhausen, M. Voges, J. Klinner, R. Schodl, C. Hassa, B. Schürmans, F. Güthe, Selected Applications of Planar Imaging Velocimetry in Combustion Test Facilities, Particle Image Velocimetry, Topics Appl. Physics, Vol 112 (2008), pp. 283-309.

15 Hamatsu

16 Sydor Instruments, Ross 2000 Streak Camera, Ross 2000 datasheet, Oct. 2015.

17 M. Gilbert, L. Davis, D. Altman, Velocity Lag of Particles in Linearly Accelerated Combustion Gases, Journal of Jet Propulsion, Vol. 25, No. 1 (1955), pp. 26-30.

18 Nootz, Gero (2012). Fit 2D Gaussian Function to Data. Retrieved April 10, 2016.

19 Oblique shock reference

20 2002 Willert